11th World Congress on Computational Mechanics (WCCM XI)
5th European Conference on Computational Mechanics (ECCM V)
6th European Conference on Computational Fluid Dynamics (ECFD VI)
E. Oñate, J. Oliver and A. Huerta (Eds)

NUMERICAL TREATMENT OF TURBULENT LOW-MACH-FLOW FOR TURBINE COOLING APPLICATIONS

S. ROCHHAUSEN*, F. KRÜPPEL† AND J. FIEDLER*

* Institute of Propulsion Technology, German Aerospace Center (DLR)
Linder Höhe, 51147 Cologne, Germany
e-mail: stefan.rochhausen@dlr.de, jens.fiedler@dlr.de
† e-mail: Florian.Krueppel@rwth-aachen.de

Key words: Separated boundary layers, Turbulence modelling, Heat transfer, Low-Mach preconditioning, Low Reynolds meshing

Abstract. In this work the performance of the DLR in-house solver TRACE is examined in simulating flow separations with heated walls compared to LES and experiments. The backward facing step has been chosen as a representative case for separated boundary layers. The purpose of the study is twofold. On the one hand, a procedure is applied to increase the convergence rate of the flow solution. On the other hand, a combination of transport models is identified that delivers accurate results for the fields of turbulent eddy viscosity and eddy conductivity.

1 INTRODUCTION

Multidisciplinary design of high pressure turbines requires a CFD tool that is able to solve the coupled system consisting of flow around and trough a turbine blade. However, the different nature of flow puts high demands on a CFD solver. The external flow around a turbine blade is typically transonic. In contrast, low Mach flows can be detected in the internal cooling channels of turbine blades. The attempt to simulate the whole turbine with cooling channels thus requires a flow solver that performs well in both types of flow, compressible transonic and incompressible subsonic flows.

Within the DLR the CFD-solver TRACE has become the standard tool for calculating flow in the main flow annulus of gas turbines. The current investigation documents the performance of TRACE in calculating internal cooling flows to be able to solve the coupled internal/external system. As a representative testcase for internal cooling channels the backward facing step has been chosen. For this testcase a broad base of numerical and experimental data exists.

The focus of this study is twofold. On the one hand, a procedure is applied to increase the convergence rate of the flow solution. On the other hand, a combination of turbulence

Table 1: Symbols and Abbreviations

c_p - specific heat capacity	ϵ - dissipation rate of k
k_θ - temperature variance	ϵ_θ - dissipation rate of k_θ
C_λ,f_λ - modelling constants (ref [7])	λ_T - eddy conductivity
Pr - molecular Prandtl number	μ_T - eddy viscosity
Pr_T - turbulent Prandtl number	ρ - density
St - Stanton number	ω_θ - specific dissipation rate of k_θ
y^+ - non-dimensional wall distance	ω - specific dissipation rate of k
β^* - modelling constant (ref [8])	

models is identified that delivers accurate results for the fields turbulent eddy viscosity and eddy conductivity.

2 FLOW SOLVER

All simulations presented in this paper have been carried out with the TRACE-code. [1] TRACE, which is developed at DLR's Institute of Propulsion Technology, is established as the DLR's standard code for turbomachinery flows. In its default configuration TRACE solves the Reynolds averaged Navier-Stokes equations in the finite volume formulation on multi-block curvilinear meshes. For the viscous fluxes a central difference scheme is used. Convective fluxes of the RANS equations are discretized by the TVD upwind scheme by Roe. For more stable and rapid convergence an implicit numerical scheme is used.

2.1 Modelling the turbulent viscosity

For modelling turbulence several models of different complexity are available in TRACE. The one-equation model of Spalart and Allmaras (hereinafter referred as 'SA') [2] is the simplest approach used in this paper. Furthermore, two different two-equations models, the Wilcox-$k\omega$-model ('Wilcox') [3] and the Menter-SST model ('Menter') [4] have been used. These models can be considered as industrial standard in the turbomachinery design process. The fourth model used in this report is the anisotropic explicit algebraic model of Hellsten ('Hellsten') [5]. The turbulence modelling approach of Hellsten is formulated on the two equation $k\omega$-basis and takes into account an extra anisotropy.

2.2 Modelling the turbulent conductivity

The most common way of modelling turbulent conductivity in modern CFD codes for turbomachinery applications is the Reynolds analogy:

$$\lambda_t = \frac{\mu_t c_p}{Pr_t} \tag{1}$$

In TRACE a constant turbulent Prandtl number $Pr_t = 0.9$ is used. Furthermore, an algebraic model according to Kays & Crawford [6] is available that varies the turbulent

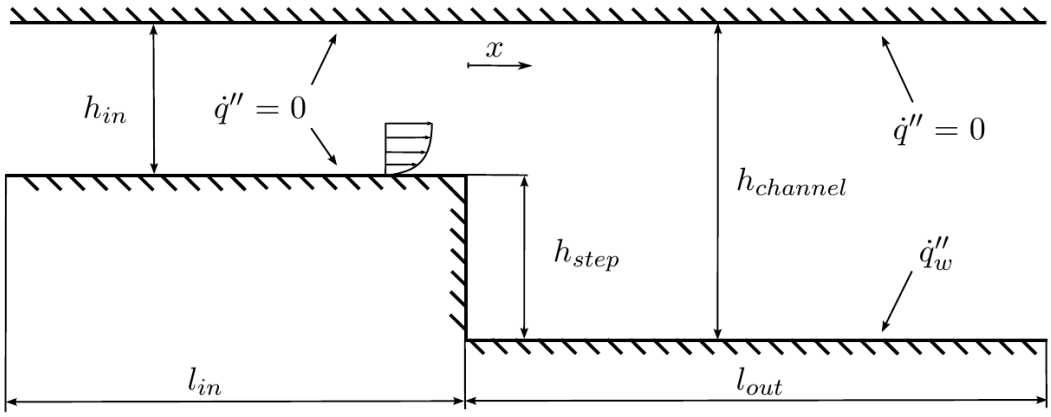

Figure 1: testcase layout

Prandtl number depending on a turbulent Peclet number.

The most complex model for turbulent conductivity in TRACE is a transport equation model. It calculates eddy conductivity λ_t from the transport equations of temperature variance k_θ and its specific dissipation rate ω_θ. This model has been derived from Nagano's $k_\theta\epsilon_\theta$-transport model [7]:

$$\alpha_t = C_\lambda f_\lambda k \sqrt{\frac{k}{\epsilon}\frac{k_\theta}{\epsilon_\theta}} \tag{2}$$

and reformulated into a $k_\theta\omega_\theta$ form. Wall damping terms are removed from the original equations [8]. The equation for the eddy conductivity yields

$$\lambda_t = \rho c_p \beta^* k \frac{1}{\sqrt{\omega\omega_\theta}} \tag{3}$$

The two equation model is formulated without using the Reynolds Analogy. Thus it should be able to calculate differences between turbulent velocity and temperature fields.

3 Testcase

The geometry investigated in this paper (see figure 1) has been chosen as a representative testcase for internal flows with boundary layer separations. Boundary conditions have been set according to experimental investigations [9], [10] and LES-calculations [11]. The inflow Reynolds number is $Re = 28000$. Boundary layer thickness upstream of the step is about 1.1 step heights. The channel expansion ratio is $\frac{5}{4}$. The wall downstream of the step is heated with a moderate constant heat flux of $\dot{q} = 270\frac{W}{m^2}$ to keep buoyancy effects small. The simulation domain is quasi two-dimensional - it consists of one cell row only.

Table 2: Mesh dependency study

Configuration	A	B	C	D	E
Total cells ($\cdot 10^5$)	0.33	0.73	1.36	2.01	8.68
y^+	0.64	0.24	0.12	0.12	0.12
$\Delta C_f[\%]$	2.1	1.3	0.2	0.1	0
$\Delta Stanton[\%]$	10	2.1	0.9	0.2	0

3.1 Meshing

Typically, low Reynolds meshes for turbomachinery applications have a first cell height around unity. Preliminary to this study a mesh dependency study has been done starting from a fine mesh with $y^+ = 0.64$ (based on a y^+-value in the developed flow upstream of the step) to even finer values. From configuration A to C the first cell height has been reduced, in configuration D and E the stretching rate has been adapted. Mesh E is the finest and has been used as a reference value. All relevant mesh-study parameters are presented in table 2.

The global maximum of Stanton number has been chosen to evaluate the influence of meshing on the heat transfer solution. No mesh dependency has been expected for wall distances y^+ lower than one. However, table 2 shows a significant difference of 10% in the global peak Stanton number between mesh A and mesh E. The global maximum of Stanton number is located at the reattachment point, where the theory of a developed boundary layer cannot be applied. In this region the wall distances differ from unity. The mesh study underlines the importance of an accurate mesh in the reattachment region in order to obtain high quality simulation results.

4 Low-Mach preconditioning

Many technical applications involve a wide range of compressible and incompressible flow regimes, e.g. cavity and seals in turbomachinery configuration. On the one hand, the application of various flow solvers for different flow speeds is computational cost-intensive. On the other hand, it is known that in density-based flow solvers the convergence history progressively degrades as the incompressibility limit (i.e. very low Mach number) is approached due to the large disparity between the acoustic and convective speeds. In order to overcome these problems several preconditioning methods are applied to the Euler as well as Navier-Stokes system of equations. Preconditioning reduces the considerable difference between the largest and smallest eigenvalue of the system. Pre-multiplication of the time derivatives by a suitable matrix diminishes the speed of the acoustic waves [12], hence yields a well-conditioned system matrix.

In this study a low preconditioning scheme previously proposed by Turkel [12] and extended and successfully tested for full three-dimensional configurations by [13] has been

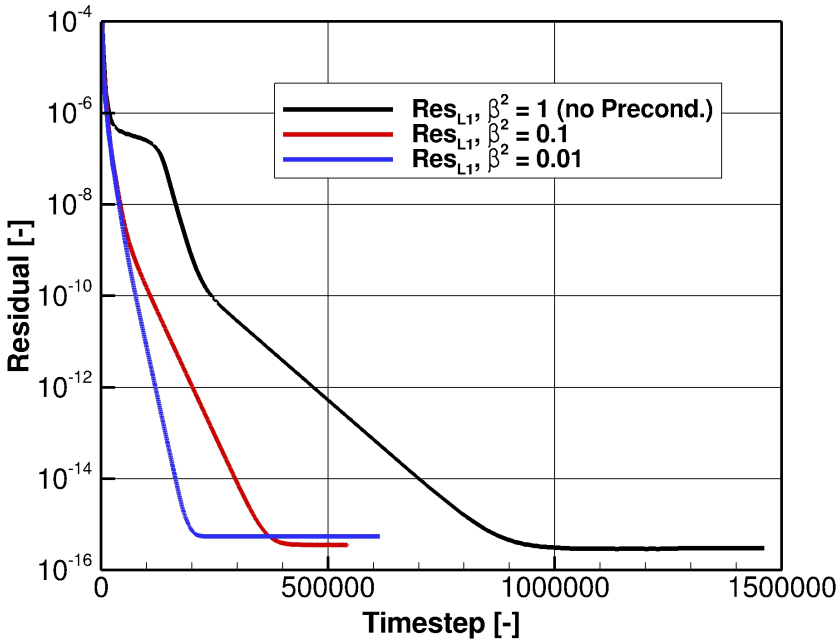

Figure 2: L_1 convergence history of a reference and low-Mach preconditioned calculation

applied to the backward facing step. Computational experiments have shown that the numerical stability is strongly influenced by a correct treatment of boundaries. This item is discussed in detail in [14]. Therefore, preconditioning is applied to the whole configuration except in the proximity of in- and outflow. In the current work the characteristics at in- and outflow are not subjected to low Mach preconditioning. Moreover, low-Mach preconditioning depends on an additional parameter, often announced to as β^2. It has been shown that this parameter has a strong impact on the quality of results and convergence acceleration. In general, β^2 is related to the local Mach number. To improve stability in the surrounding of unmodified boundaries tests have been performed taking a constant preconditioning parameter into account.

In figure 2 the convergence histories of a reference calculation compared to computations under the auspices of low-Mach preconditioning are presented. As clearly shown, the preconditioned calculations reach machine precision much faster than without preconditioning. The influence of a variable determined β^2 on the current configuration will be the focus of a future work.

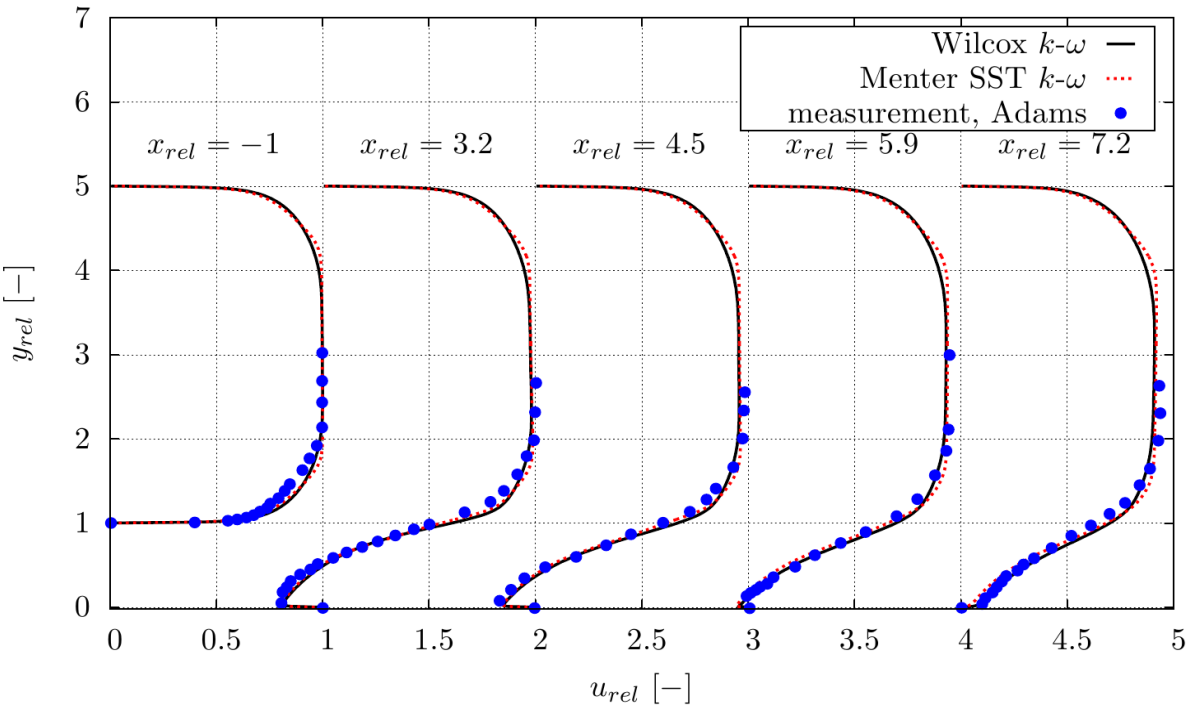

Figure 3: Velocity plots Wilcox & Menter 1

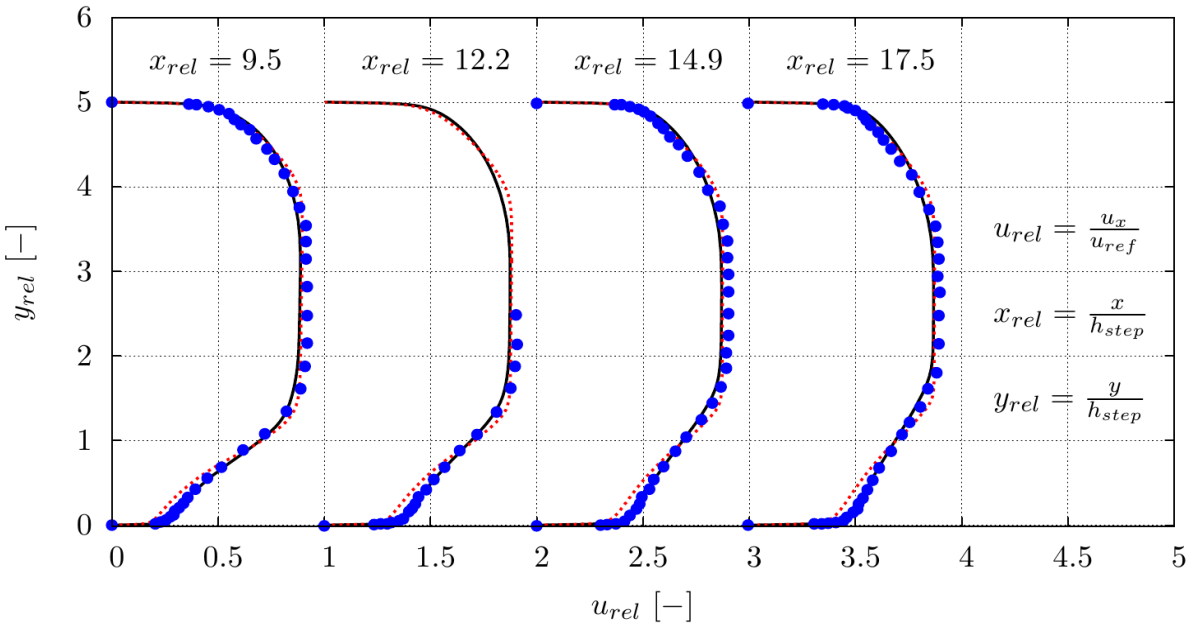

Figure 4: Velocity plots Wilcox & Menter 2

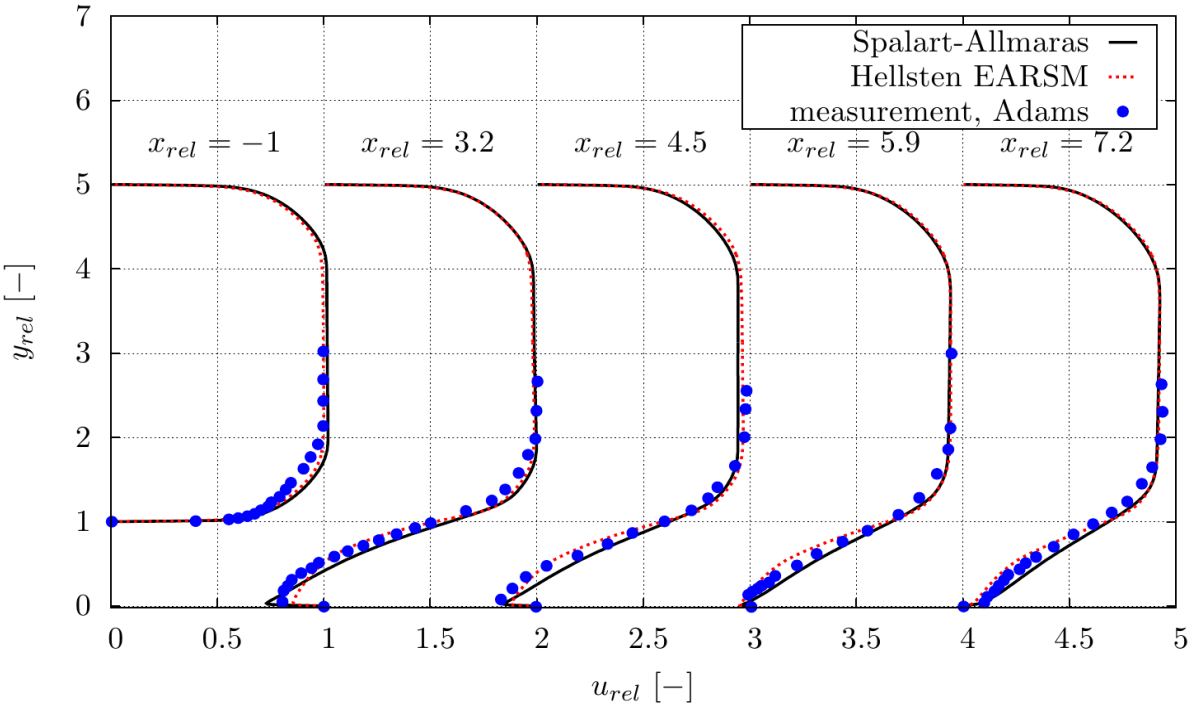

Figure 5: Velocity plots Hellsten & SA 1

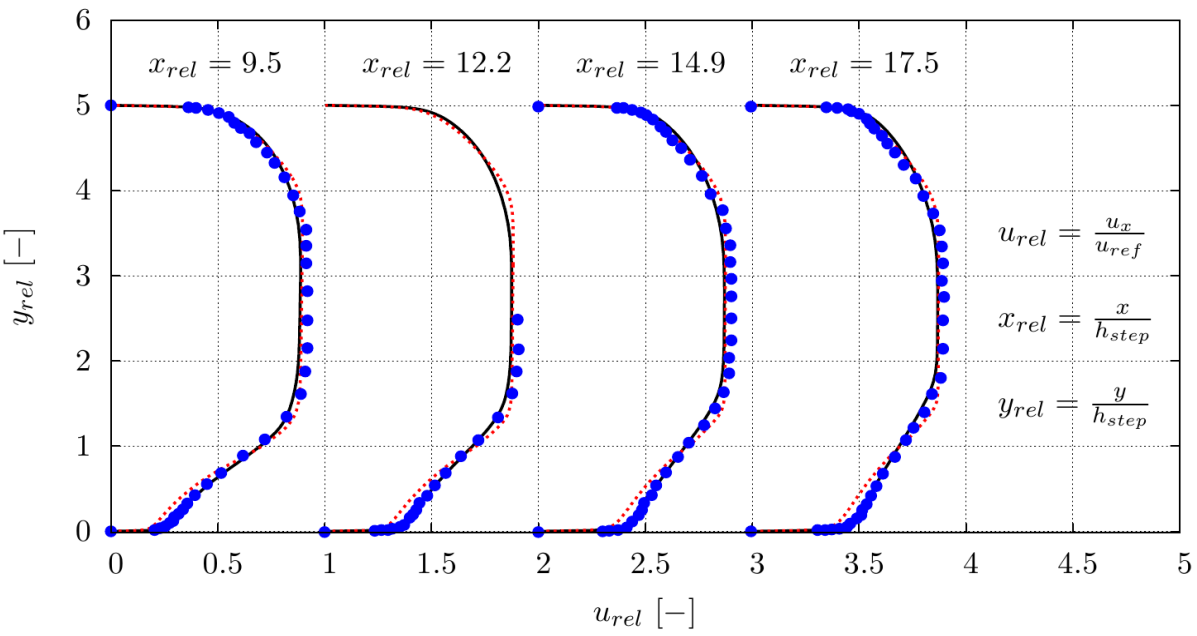

Figure 6: Velocity plots Hellsten & SA 2

5 Results

5.1 Calculations using Reynolds Analogy

In figure 3 and 4 the velocity fields of the Wilcox and Menter models are plotted. At positions $x_{rel} = -1$ to $x_{rel} = 7.2$ no significant differences occur between RANS simulations and the experimental data. Starting from position $x_{rel} = 9.5$ the simulation with Menter predicts less steep velocity gradients compared measurements and Wilcox calculations.

Figures 5 and 6 show velocity fields of SA and Hellsten. Position $x_{rel} = 3.2$ is located in the center of the recirculation area, here the differences between Hellsten and SA are obvious. Whilst Hellsten predicts a rounder velocity profile with a maximum recirculation velocity lower than measured, SA predicts a sharper profile with a higher recirculation velocity than measured. *From position $x_{rel} = 9.5$ downstream EARSM behaves like SST?*

In figure 7 the friction coefficient is plotted for the lower sidewall. All models indicate a reattachment point at roughly seven step heights. Downstream of this point the models performance differs. The models of Hellsten and Wilcox predict higher c_f-values than measured, SA, in contrast, predicts lower values. Calculations with the Menter model are in good agreement with LES-calculations and measurements. Upstream of the reattachment point only two equation Menter and Wilcox models show agreement in the minimum c_f-value which is located at approximately x_{rel}=4.

Figure 8 shows heat transfer coefficients for the lower sidewall plotted against x_{rel} for all four eddy viscosity models using Reynolds analogy. Maximum heat transfer rates are located slightly upstream of reattachment. Downstream of the Stanton number maximum Wilcox and Menter simulations are in good agreement with measurements and LES data. Hellsten modelling predicts too high and SA modelling predicts too low heat transfer rates. Moreover the SA model predicts an small increase in heat transfer from $x_{rel} = 10$ downstream which is non-physical in a fully turbulent boundary layer.

The heat transfer rate deviations result from the coupling of eddy conducivity and eddy viscosity via Reynolds analogy - models that predict to low c_f-values simulate too low heat transfer rates and vice versa.

5.2 Beyond Reynolds Analogy

For the calculations with non-adiabatic walls the Menter model has been chosen. This model shows the best agreement between measurements of wall shear stress and heat transfer rates downstream of reattachment.

Figure 9 shows Stanton numbers calculated with different modelling strategies for eddy conductivity calculation. The predicted global peak heat transfer rate differs. The assumption of a constant Prandtl number leads to the highest coefficient, the $k_\theta\omega_\theta$-model predicts the lowest. Upstream of $x_{rel} = 2$ the differences between the three different eddy conductivity models almost vanish. Figures 8 and 9 show clearly the importance of simulating accurately the maximum global heat transfer rate since it also determines the rates

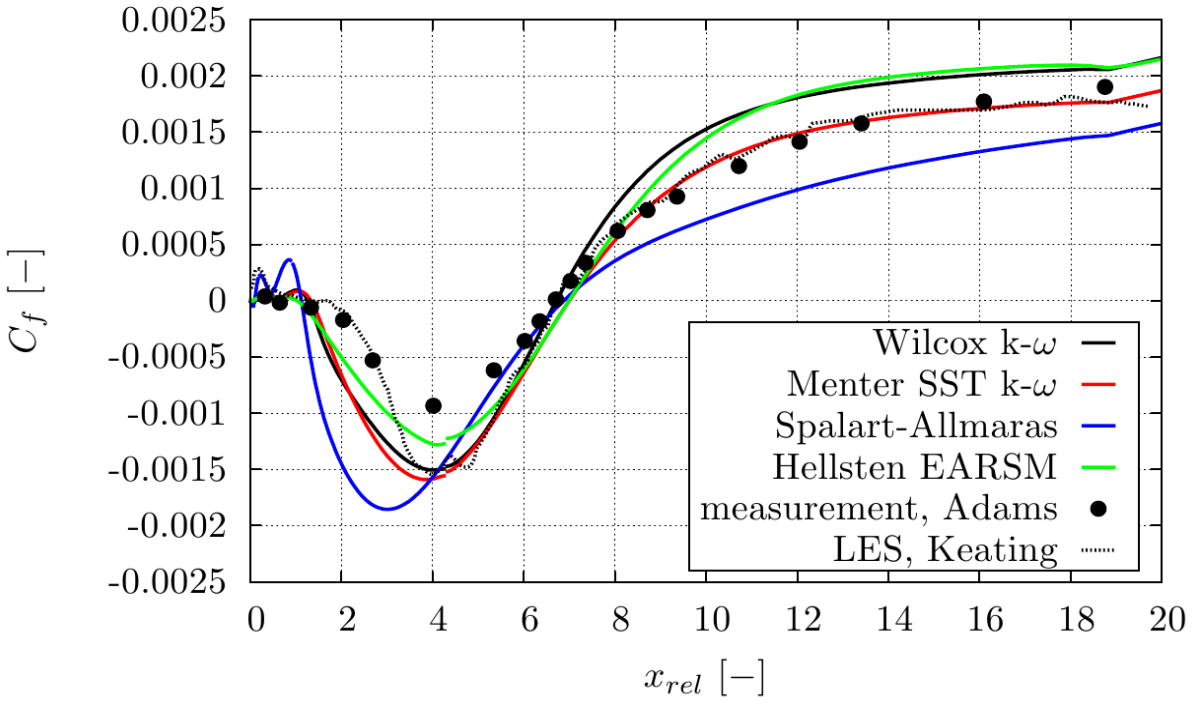

Figure 7: Friction coefficients for simulations using Reynolds analogy

further downstream.

In the region between $x_{rel} = 0$ and $x_{rel} = 1$ heat transfer rates differ up to 60% between the RANS, LES and experimental data. The explanation can be found in the mesh. In this investigation a mesh with a sharp edge between the step wall and the heated lower wall is used. This leads to a fractal structure of a vortex and a smaller counterrotating vortex. The oscillations in the friction coefficient can be observed in figure 7. The occurrence of these small scale vortices strongly on the turbulence model used. However, due to the lack of sufficient measurement points no statement can be made about modelling accuracy compared to experimental data.

It can be summarized that all three modeling assumptions for turbulent viscosity model the heat transfer rate in good agreement with experiments. The algebraic model gives the best predictions compared to the experiment. The $k_\theta\omega_\theta$-model needs a further calibration in order to better predict maximum heat transfer rate in the reattachment region.

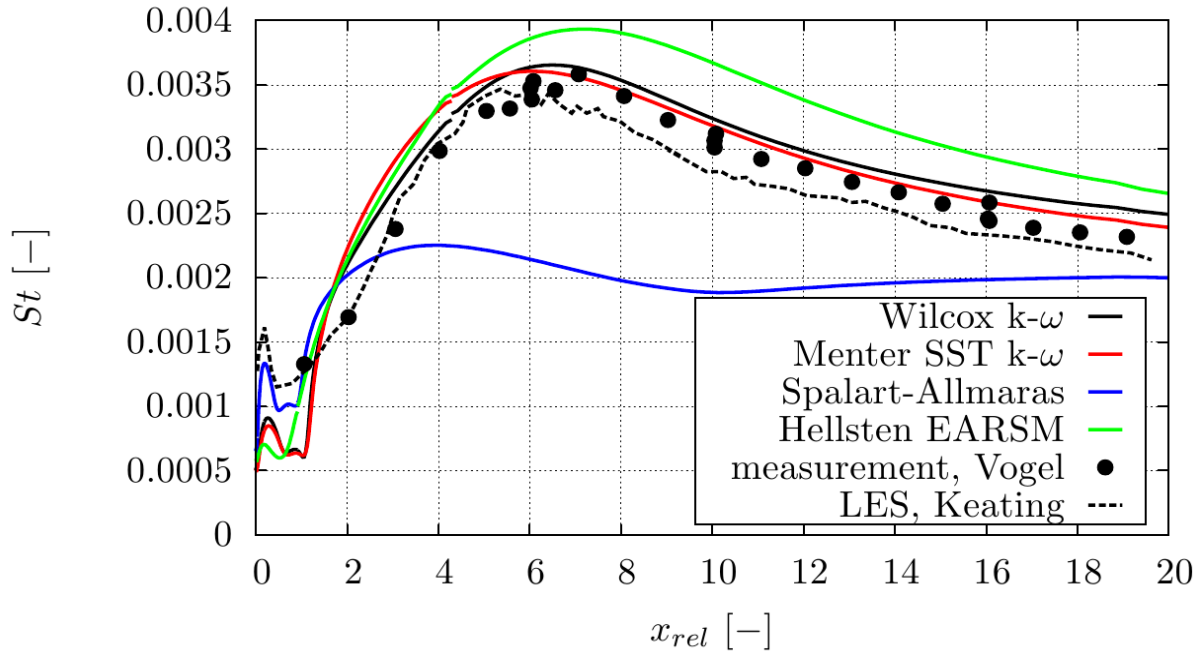

Figure 8: Stanton numbers for simulations using Reynolds analogy

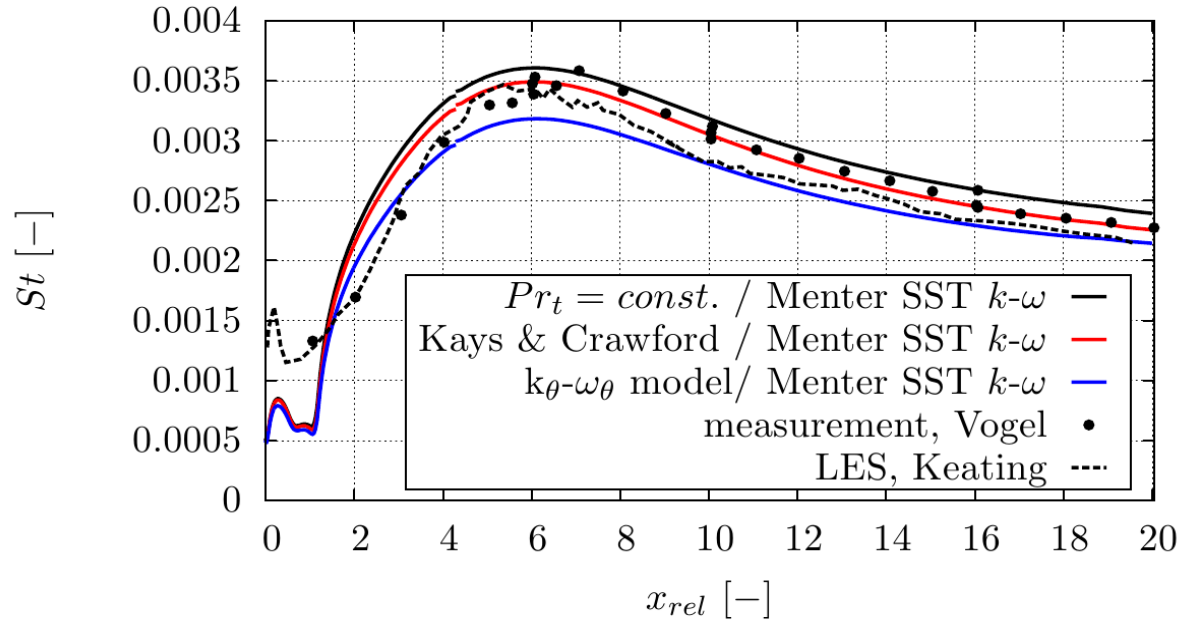

Figure 9: Stanton numbers for simulations using different turbulent heat transfer modelling

6 CONCLUSIONS

The backward facing step has been investigated with the RANS code TRACE. Seven different turbulence models of different closure level have been applied; four transport

models for turbulent viscosity, three strategies of modelling the turbulent conductivity. Computational results have been compared to results obtained by a LES calculation and experimental data. Due to the low flow speed a numerical procedure is applied to increase the convergence.

To sum up:

- The preconditioning algorithm strongly increases the convergence rate compared to reference calculations
- All turbulence models can reproduce the reattachment point
- The models performance differs significantly in the recirculation area
- Best overall flow field prediction has been achieved with Menter SST
- Heat transfer rate predictions are in good agreement with the experimental results in proximity of the reattachment point and further downstream

For future investigations it might be helpful to perform calculations with Hellsten and $k_\theta\omega_\theta$-modelling to overcome the rigid coupling of eddy conductivity and eddy viscosity. Also high resolution temperature field measurements could help in the improvement of transport models predicting eddy conductivity, certainly in the proximity of the step.

REFERENCES

[1] Becker, K., Heitkamp, K., and Kügeler, E., Recent Progress In A Hybrid-Grid CFD Solver For Turbomachinery Flows, *V European Conference on Computational Fluid Dynamics* (ECCOMAS CFD 2010) , Lisbon, Portugal, June 2010.

[2] Spalart, P. and Allmaras, S., A one-equation turbulence model for aerodynamic flows. *La Recherche Aerospatiale* (1992) **1**:5–21

[3] Wilcox, D. C. *Turbulence Modeling for CFD.* DCW Industries, La Cañada, USA, Vol. III., (2006).

[4] Menter, F. R., Two-equation eddy-viscosity turbulence models for engineering applications. *AIAA journal* (1994) **32**:1598–1605

[5] Hellsten, A. K., New Advanced kw Turbulence Model for High-Lift Aerodynamics. *AIAA journal* (2005) **43**:1857–1869.

[6] Crawford, M. E., Kays, W. M. *Convective Heat and mass transfer.*McGraw-Hill. (1993).

[7] Nagano, Y. and Kim, C., A two-equation model for heat transport in wall turbulent shear flows. *J. Heat Transf.* (1988) **110**:583–589

[8] Rochhausen, S., Reformulation of a two-equation model for the turbulent heat transfer. *Proceedings of the Seventh International Symposium on Turbulence, Heat and Mass Transfer Palermo, Italy* (THMT 2012)

[9] Vogel,J. C., Heat transfer and fluid mechanics measurements in the turbulent reattaching flow behind a backward-facing step. *PhD Thesis , Stanford University* (1984)

[10] Adams, E.W., Experiments on the structure of turbulent reattaching flow. *PhD Thesis , Stanford University* (1984)

[11] Keating, A. and Piomelli, U. and Bremhorst, K. and Nesic, S., Large-eddy simulation of heat transfer downstream of a backward-facing step. *J. Turbul.* (2004) **5**

[12] E. Turkel, Preconditioned methods for solving the incompressible low speed compressible equations., *J. Comput. Phys.* (1987) **72**:277–298

[13] J. Fiedler and F. di Mare, Generalised Low-Mach preconditioning for arbitrary three-dimensional geometries. *European Congress on Computational Methods in Applied Sciences and Engineering* (ECCOMAS 2012)

[14] J. Fiedler and F. di Mare, Low-Mach preconditioned boundary conditions for compressible solvers. *Proceedings of the 6th European Congress on Computational Methods in Applied Sciences and Engineering* (ECCOMAS 2014)